Application note

Analysis of DNA melting through UV-Visible absorption spectroscopy

Effect of base-pair mismatch and solvent environment

Introduction

Deoxyribose nucleic acid (DNA) is a naturally occurring polymer made up of four unique nucleic acid subunits (thymine, adenine, cytosine, and guanine) referred to as "bases." When connected through a phosphate sugar backbone, a single DNA strand is formed. The bases which make up single-stranded DNA (ssDNA) can associate or "pair" with bases on a separate ssDNA sequence through hydrogen-bonding interactions. The most common pairing structure, Watson-Crick, consists of two hydrogen bonds between thymine and adenine and three hydrogen bonds between cytosine and guanine,[1] as shown in Figure 1. Once paired in this manner, the newly formed double-stranded DNA (dsDNA) forms the well-characterized double-helix secondary structure.

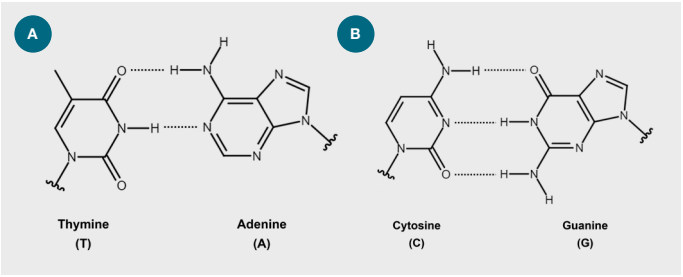

Figure 1: Hydrogen bonding interactions between (a) adenine and thymine and (b) cytosine and guanine Watson-Crick base pairs.

DNA serves as a template by which other materials are derived and has been used in a myriad of pharmaceutical applications, including gene therapy and vaccine development, among others.[2–5] In these uses, the makeup of the sequence is integral for the synthesized material to perform as intended, requiring analysis and confirmation of the overall composition. DNA melting experiments can be particularly useful for understanding the structure of the material and has previously been used to study gene expression.[6]

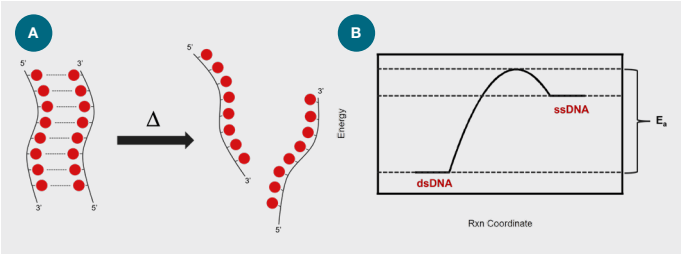

Figure 2: Depiction of the formation of single stranded DNA (a) and a general energy diagram for the DNA melting process (b) where Ea is the activation energy of the system.

DNA melting, or denaturation, describes the process under which dsDNA disassociates into its single-stranded components (Figure 2a and equation 1).

$$dsDNA \leftrightarrow 2ssDNA \quad (1)$$

As described previously, dsDNA is held together through hydrogen bonding interactions between the base pairs within the sequence (Figure 1). To form ssDNA, these interactions must be broken, and the system must exist in conditions which thermodynamically favor ssDNA over ddDNA. Considering thermodynamics, an energy activation barrier must be overcome to push the system towards the formation of ssDNA from dsDNA (Figure 2b). The energy needed to overcome this barrier is specific to the composition of the DNA sequence, and as such, can serve as a useful analysis method for probing DNA structure. The transition from dsDNA to ssDNA can occur when the system is elevated to higher temperatures. By introducing heat, the energy of the system increases, providing the energy needed to transition from dsDNA to ssDNA.[7] By convention, the melting temperature (T_m) is defined as the temperature at which half of the dsDNA has denatured.[1,8]

DNA has previously been well characterized through spectroscopic methods and is known to absorb in the UV spectral region, with an absorption maximum of 260 nm.[9] This absorption feature comes from π → π* transitions related to the p-orbitals on the purine or pyrimidine aromatic ring.[8,9] When in the double helix structure, the hydrogen bonds disrupt the resonance structure of each base, decreasing the strength of the π → π* transition. This weaker transition results in a smaller extinction coefficient (ε) for the overall structure. From Beer's law,

$$A = cl\varepsilon \quad (2)$$

where A is the measured absorbance, c is the concentration of the analyte, and l is the path length, a smaller ε will result in a lower observed absorbance for the dsDNA compared to the ssDNA. Consequently, by monitoring the observed change in absorption at 260 nm as a function of temperature, we can observe the point at which half of the dsDNA has disassociated into its single-stranded components. As UV-Visible absorption spectroscopy is a non-destructive technique, this analysis can be carried out using samples which can be further analyzed later.

In an ideal scenario, the resulting sigmoidal curve, as shown in Figure 3, should be observed, where no change is observed at low temperatures (where dsDNA is favored), a steep change in absorption in the melting temperature region and a second region where absorbance is constant (where ssDNA is favored). The inflection point of this curve will correlate to the melting temperature of the DNA sample.

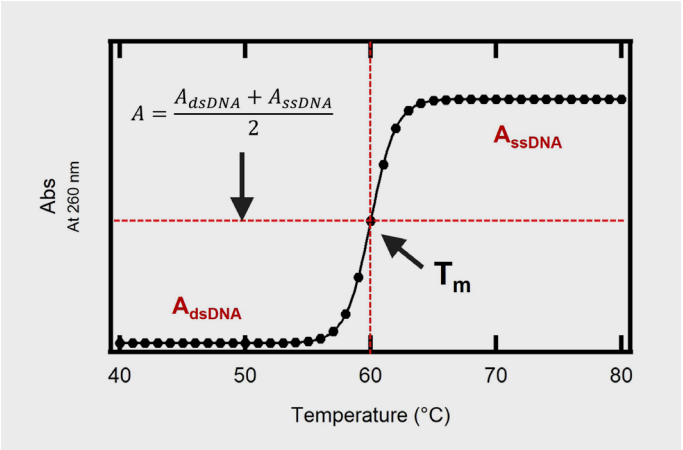

Figure 3: Ideal DNA melt curve. A_{dsDNA} corresponds to the absorption due to dsDNA, and A_{ssDNA} refers to the absorption due to ssDNA. T_m is the melting temperature, defined as the point at which half of the dsDNA is in the single-stranded form.

As described previously, melting temperature is specific to the sequence of DNA. For example, the amount of GC base pairs present in the double-stranded structure will inherently require more energy, and consequently a higher melting temperature.[10] This arises as GC pairs involve three hydrogen bonds as opposed to the two hydrogen bonds needed for AT pairs (Figure 1). The nearest neighbor bases, which are "stacked" with bases above and below in the strand, can also influence the melting thermodynamics through additional stabilizing interactions, influencing the melting temperature.[9,11] Additionally, any non-traditional secondary structure, including i-motif,[12] will also impact the melting temperature, as well as mutations within the structure which result in no pairing between bases (ex: base-pair mismatch).[13]

Beyond structural effects, the solvent environment, including added compounds, can also influence the melting temperature and must be considered when performing melting experiments. These effects include the effect of buffer conditions/salt concentration, which can stabilize the dsDNA secondary structure, requiring a higher temperature to effectively denature the material.[14,15] Compounds in solution which can bind to DNA, such as fluorescent probes, can also change the melting temperature.[16] Consequently, it is important to consider not only the makeup of the DNA sequence itself, but the interactions the DNA can have with various components present in the solvent as well when analyzing melting temperature.

Herein, the melting temperature for both small (40 base pairs per strand) and large (~2,000 base pairs per strand; calf thymus) dsDNA sequences was determined. Absorption measurements were obtained using a Thermo Scientific™ Evolution™ One Plus UV-Visible Spectrophotometer equipped with the Quantum Northwest t2 Sport Peltier cuvette holder to change the temperature of the sample. The melting temperature was calculated within the Thermo Scientific™ Insight™ Pro Software. As described earlier, the melting temperature is sensitive to a variety of factors, including changes to the solvent environment and DNA structure. Consequently, additional experiments were performed to demonstrate the effect of base-pair mismatch, dye binding, and salt concentrations on the melting temperature.

Experimental

Materials and sample preparation

Four 40 base-pair long DNA strands were purchased through Integrated DNA Technologies and are described in Figure 4. Seq. 1–3 are nearly identical; however, 3 bases were changed for Seq. 2 and 6 were changed for Seq. 3. Each ssDNA sample was reconstituted with tris-EDTA (TE) buffer (1X, pH 7.4) to achieve a concentration of 10 ng/µL. Equivalent proportions of the

Seq. 1 – 0 base-pair mismatch

5' – ATT CGT GCA ACG ATG TAC AGT TTA ACC GTA TGC AGA TTC C – 3'

Seq. 2 – 3 base-pair mismatch

5' – ATT CGT GTA ACA ATG TAC AGT TTA ACC GTA TGC AGA TTC C – 3'

Seq. 3 – 6 base-pair mismatch

5' – ATT CGT GTA ACA ATG TAC AGT TTA ACC GCA TGA AGA GTC C – 3'

Complement

5' – GGA ATC TGC ATA CGG TTA AAC TGT ACA TCG TTG CAC GAA T – 3'

Figure 4: 40 base-pair ssDNA sequences.

appropriate sequence (Seq. 1, 2, or 3) and the complement were then mixed together and diluted with TE to ensure the same concentration of each strand was present in the solution. A total of three dsDNA solutions were made, each using the same complement strand with different sequences (Seq. 1–3).

The samples were then annealed by raising the temperature of the solution to 90 ˚C, and then cooling back down to room temperature (~25 ˚C), ensuring the sequences were able to form the typical double helix structure. For the melting experiments performed using an absorption spectrophotometer, each solution was diluted again with TE to a concentration of 3.8 ng/µL.

For fluorescence measurements, the SYBR® Select Master Mix (2X), referred to as SYBR Green in the text, was used as a fluorescent probe. For each sample sequence, 40 µL of the SYBR Select Master Mix (2X) was added to 20 µL of 10 ng/µL of the appropriate dsDNA sample. Each sample was further diluted using 20 µL of TE buffer. The samples were then split into three replicate samples, each 20 µL in total volume and loaded into a 96 well plate.

Calf thymus DNA samples were made using Invitrogen™ UltraPure™ Calf Thymus DNA solution (Lot # 2411666). A 200 ng/µL stock solution was made by diluting the calf thymus solution with TE buffer. The NaCl stock solution was made by dissolving 0.29 g NaCl in 10 mL of TE buffer solution (500 mM NaCl). Two separate NaCl solutions were then made with concentrations of 5 mM and 10 mM.

For the melting experiments, the control sample was prepared by diluting 100 µL of 200 ng/µL calf thymus with 1.9 mL of TE buffer to achieve a final concentration of 10 ng/µL. Two more 10 ng/µL calf thymus samples were made using the 200 ng/µL calf thymus stock solution, however they were instead diluted using the NaCl + TE buffer solutions as described in Table 1.

Thermo Scientific Evolution Spectrophotometers

Instrumentation and experiment parameters

For all absorption experiments, the Evolution One Plus UV-Visible Spectrophotometer was used to collect the absorption of each sample at 260 nm. The Quantum Northwest t2 Sport Peltier accessory was used to control the temperature of the sample. The bandwidth was set to 1.0 nm, a 1.0 s integration time, and a 1.0 s dwell time was used. The temperature ramp was set to three different stages as described in Table 2. These temperature ramps were set such that more points could be collected in the range spanning the anticipated melting region. The final stage was used to cool the solution back down to room temperature.

All temperature measurements were collected using a temperature probe and read through Insight Pro Software. The probe was suspended in the solution using a Teflon® cuvette cap, preventing the probe from touching the cuvette walls and limiting the loss of solvent from evaporation. The use of a temperature probe is vital as the heat from the Peltier accessory will not transfer to the sample instantaneously. Additionally, all absorption measurements were collected while the solution was stirred using a small stir bar. This aids in preventing bubbles from sticking to the sides of the cuvette, which can influence the measured absorbance, and ensures the heat is dispersed throughout the cuvette evenly.

For fluorescence measurements, an Applied Biosystems™ QuantStudio™ 6 Pro PCR system was used. Each sample was run in triplicate and held in the appropriate 96 well plate, capable of allowing UV light to pass through. The samples were then heated to 95 ˚C within 15 seconds, cooled back down to 40 ˚C for 1 min and finally heated back up to 95 ˚C for 5 seconds. Fluorescence measurements were collected every 0.3 ˚C.

Table 1: Sample preparation concentrations and amounts for calf thymus with and without NaCl present.

Sample	Volume of 200 ng/µL calf thymus (µL)	Buffer solution		[NaCl] in sample (mM)
		[NaCl] in TE buffer (mM)	Volume of buffer added (mL)	
1	100	0.0	1.9	0.0
2	100	5.0	1.9	4.8
3	100	10.0	1.9	9.5

Table 2: Temperature ramp parameters for melting experiments performed using the Evolution One Plus Spectrophotometer equipped with the Quantum Northwest Peltier accessory.

Stage	Final temperature (˚c)	Ramp rate (˚c/second)	Hold time (seconds)	Measurement interval (seconds)
1	40	0.0833	2	30
2	95	0.0167	15	30
3	25	0.0833	0	N/A

Melting temperature analysis methods

Practically, the melting temperature of an ideal system, as shown in Figure 3, can be determined through a "horizontal-intercept" method. In this analysis, the dsDNA and ssDNA temperature regions are fit to two separate linear functions which do not depend on the melting temperature, only varying in the y-intercept. The average of the two linear functions for the dsDNA and ssDNA regions is then determined and the intersection between this average linear function and the melt curve is taken. This point corresponds to the melting temperature of the sample.

For most DNA samples, the absorbance will likely vary outside of the melting region, preventing the use of the horizontal intercept analysis method. Instead, two alternative methods can be used: the "slope-intercept" and "inflection" methods. In the slope-intercept analysis, similar to the horizontal intercept analysis, the temperature ranges before and after the melting temperature regime are fit to two different linear functions with dependence on the temperature (y=mx+b). Typically, the slope of these functions will be the same. The average of the two functions is then determined and the intersection of the average linear function and the melt curve is reported as the melting temperature.

However, for DNA melt curves which deviate greatly from ideal behavior or contain multiple melting temperature ranges which overlap, the inflection method is most appropriate. In this method, the first derivative of the melt curve is obtained. Mathematically, the inflection point of a function will be the maximum of the first derivative of the initial function. As the inflection point of the melt curve correlates to the melting temperature, the maximum of the first derivative can be used to easily find the melting temperature(s) in a more complex system.

All three of the outlined analysis methods are available through the Insight Pro Software. In the absorption measurements described herein, either the slope intercept or inflection method was used as the collected melt curves did not display ideal behavior. For the fluorescence measurements, the melting temperature was determined using the inflection method.

Results and discussion

Effect of base-pair mismatch

As described previously, melting temperature is highly dependent on the makeup of the DNA sequence, including the presence of mutations. This sensitivity to deviations from the anticipated sequence makes this analysis a useful check prior to further processing and scale-up. To highlight this principle, the melting temperature was determined for three dsDNA sequences consisting of 40 bases per strand with varying amounts of mismatched bases (Figure 5). Melting temperatures were determined using the slope-intercept method described previously and are reported in Table 3.

The control DNA sample with no base-pair mismatches was found to have a melting temperature of 58.4 ˚C (Figure 5b). By introducing only 3 mismatches to one end of the 40 base-pair DNA structure (Figure 5c), the melting temperature was lowered by ~6 ˚C. When 3 additional base-pair mismatches were included on the opposite end of the DNA (Figure 5d), the melting temperature was lowered again. For the DNA sample with 6 base-pair mismatches, the melting temperature was found to be ~14 ˚C lower than the control sample. With the loss of traditional base pairing, these mismatched regions are not expected to be held together through hydrogen bonding, further lowering the energy needed to denature and, therefore, the temperature needed to form stable ssDNA in solution. Consequently, with more mismatches, the melting temperature should lower, as is observed in Figure 5.

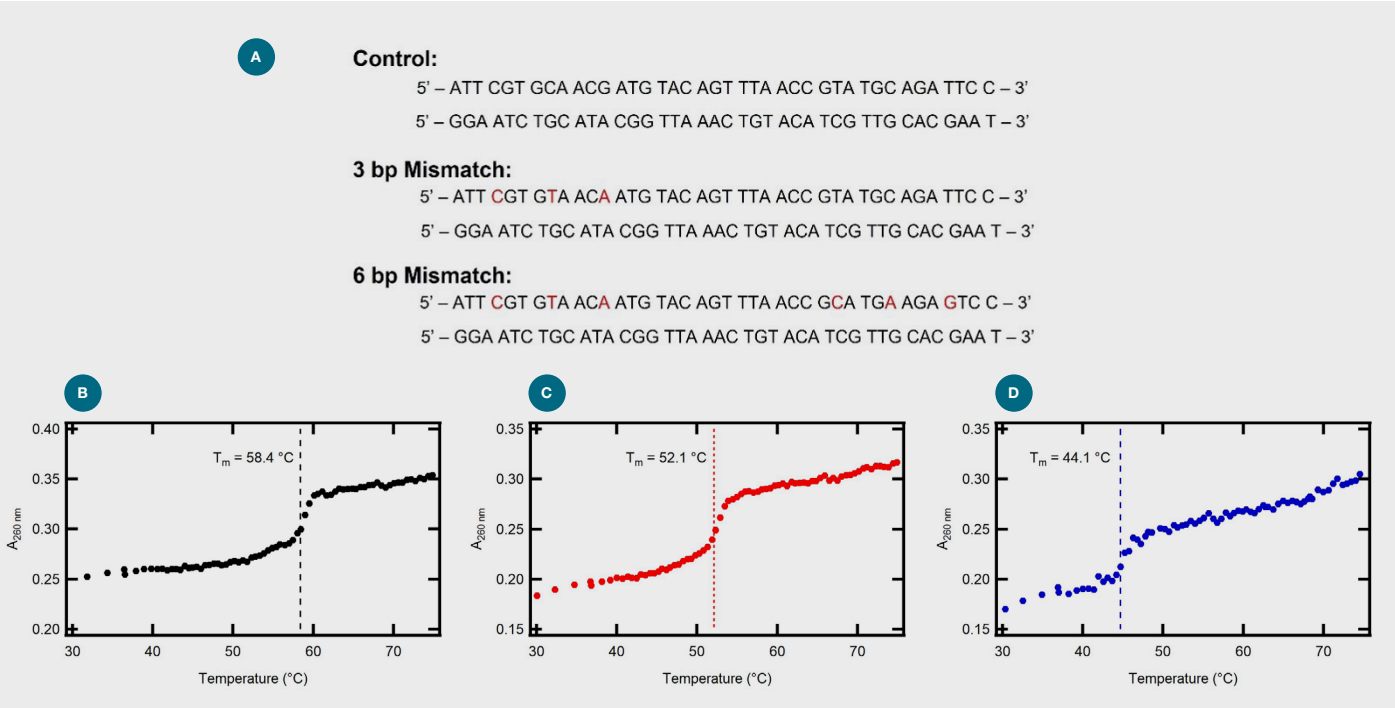

Figure 5: (a) DNA sequences with and without base-pair mismatches. Absorption vs temperature melting curves for 40 base-pair DNA sequences (3.8 ng/mL in TE buffer) with (b) 0, (c) 3 and (d) 6 base-pair mismatches. Vertical lines correspond to the calculated melting temperature. Melting temperatures were determined using the sloped intercept analysis.

Effect of bound compounds

Absorption is not the only experimental method by which the melting temperature of a dsDNA sequence can be determined. Alternatively, fluorescence spectroscopy can be employed. In this analysis, a fluorescence dye that can interact with the dsDNA is added to the sample. For example, SYBR Green (Figure 6b) is known to bind to the minor groove of dsDNA.[17] When bound, a fluorescence signal is observed. Once the DNA denatures, SYBR green is no longer bound to dsDNA and will not be fluorescence, resulting in a similar melting curve as seen for absorption-based melting temperature measurements.

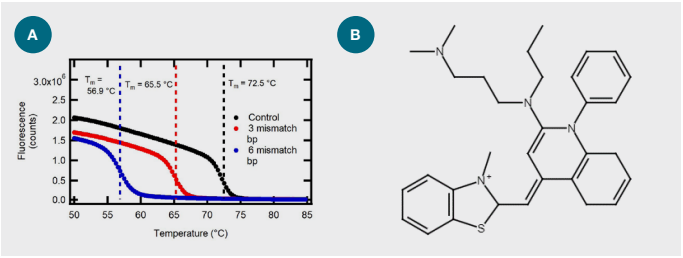

Figure 6: (a) Fluorescence vs. temperature melting curves of three 40 base-pair DNA sequences (black—0 base-pair mismatch, red—3 base-pair mismatch, and blue—6 base-pair mismatch) each coupled with SYBR green as a fluorescent probe. (b) SYBR Green I structure.

This fluorescence method was used to analyze the melting temperatures of the three 40 base-pair DNA sequences previously studied using UV-Visible absorption (Figure 6a). The melting temperature was determined through the inflection method. As shown in Figure 5, the same trend in melting temperature was observed in which dsDNA with more base-pair mismatches demonstrated a lower melting temperature compared to the control. However, as shown in Table 3, the melting temperature determined through this fluorescence analysis is between 12–14 ˚C higher than what was observed through the UV-Visible absorption method. This discrepancy in melting temperature is not a result of the technique used but is instead a result of the presence of SYBR Green in the sample solution.

Table 3: Calculated melting temperatures for three separate 40 base-pair dsDNA samples using both absorption and fluorescence-based methods where the latter used SYBR Green as a fluorescent probe.

Number of base-pair mismatches	T_m (˚C)	
	Absorption method	Fluorescent probe method
0 (control)	58.4	72.5
3	52.1	65.5
6	44.1	56.9

As SYBR Green is bound to the dsDNA in solution, it serves almost as a linker between the dye and the dsDNA. The interactions which hold SYBR Green to the minor groove of the DNA must also be broken before the DNA can denature into single strands. The raised melting temperature reflects the extra energy needed to effectively separate the two strands from one another in the presence of a bound dye. If using the fluorescent probe method, it is important this binding interaction be considered when estimating the melting temperature of the DNA sequence of interest. However, as the UV-Visible absorption method only relies on the DNA itself and not the introduction of an additional probe/bound compound, this technique will provide a better measurement of the melting temperature.

Effect of salt concentration

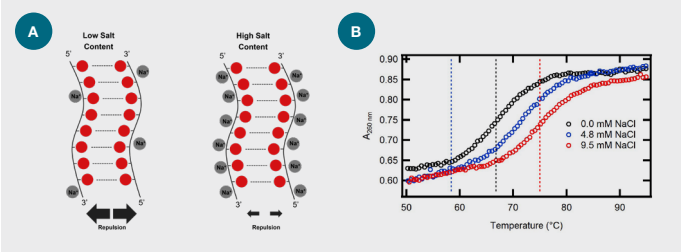

Figure 7: (a) Absorption vs. temperature melting curves for 10 ng/µL calf thymus DNA suspended in TE buffer and varying concentrations of NaCl (black—0 mM NaCl, blue—4.8 mM NaCl, and red—9.5 mM NaCl). Vertical lines denote the calculated melting temperatures (T_m) for each sample included. (b) Depictions of the effect of salt concentration on strand repulsion.

While fluorescent probes influence melting temperature through binding to the minor groove of the DNA double helix, the presence of ions in solution can also influence the measured melting temperature. Figure 7 includes the melting curves collected for three separate calf thymus DNA samples. Melting temperatures were determined through the inflection method. The three samples vary in concentration of excess salt (0 mM, 4.8 mM, and 9.5 mM NaCl). As shown, increasing the concentration of NaCl results in an increase in the melting temperature of dsDNA from 66.8 ˚C with no NaCl added to 75.0 ˚C with 10 mM NaCl present in the solution (Table 4).

In this example, the effect the presence of salt has on the backbone must be considered. The phosphate group on the sugar backbone provides the net negative charge for ssDNA. Though the hydrogen bonding interactions are strong enough to hold dsDNA in the double helix structure, the close proximity of the two negatively charged DNA strands will result in some repulsion. Consequently, this behavior will push the equilibrium towards the formation of ssDNA, which in turn lowers the energy and temperature needed to denature the dsDNA.

Table 4: Melting temperatures for calf thymus DNA with varying concentrations of NaCl.

DNA sample	[NaCl] (mM)	T_m (˚C)
Calf thymus	0.0	66.8
	4.8	71.6
	9.5	75.0

When positively charged ions, like Na^+, are present in solution, they can associate with the negatively charged phosphate groups on the DNA backbone providing stabilization of the dsDNA structure. These ions will effectively screen the charge of the two DNA strands, thereby lowering the repulsive forces between them. As the repulsion is lowered, the energy barrier for forming ssDNA will rise, requiring a higher temperature to denature dsDNA. If the concentration of positively charged ions present is increased, the repulsive forces will continue to reduce until there are enough positively charged ions added

to produce a net neutral charge. As buffers, like tris-EDTA, will also stabilize the backbone in much the same manner, changes in the concentration of the buffer components can also influence how stable the DNA is in solution and, in turn, the melting temperature. Therefore, it is vital to ensure solvent conditions are considered and must be kept consistent when comparing melting curves from multiple DNA samples.

Conclusions

Determining the melting temperature of dsDNA can be a useful tool for analyzing the composition and structure of the sample. Specifically, this analysis can allow for the identification of irregularities in the DNA sequence, including base-pair mismatches, and can lead to a better understanding of the environmental effects. As a result of the sensitivity of this technique to the solvent, special care should be taken to account for variations based on the environment, as opposed to changes in the sequence structure/composition.

Through UV-Visible absorption spectroscopy, this property of a dsDNA sample can be determined by non-destructive means, allowing for further types of analysis to be performed on the same samples at a later time. The Evolution UV-Visible Spectrophotometers, including the Evolution One Plus instrument used for the above experiments, coupled with the Quantum Northwest t2 Sport Peltier system, can perform these measurements easily. Additionally, the Insight Pro Software is able to calculate the melting temperature with ease, minimizing the data work-up needed post-collection.

References

1. Khandelwal, G.; Bhyravabhotla, J., A Phenomenological Model for Predicting Melting Temperature of DNA Sequences, *PLoS ONE*, **2010**, 5, e12433.
2. Liu, M.A., DNA Vaccines: A Review, *J. Intern. Med.*, **2003**, 402–410.
3. Patten, P.A.; Howard, R.J.; Stemmer, W.P.C., Applications of DNA Shuffling to Pharmaceuticals and Vaccines, *COBIOT*, **1997**, 8, 724–733.
4. Pardoll, D.M.; Beckerleg, A.M., Exposing the Immunology of Naked DNA Vaccines, *Immunity*, **1995**, 3, 165–169.
5. Richardson, B., DNA Methylation and Autoimmune Disease, *J. Clin. Immunol.*, **2003**, 109, 72–79.
6. Jeong, S.; Hahn, Y.; Rong, Q.; Pfiefer, K., Accurate Quantitation of Allele-Specific Expression Patterns by Analysis of DNA Melting, *Genome Res.*, **2007**, 17, 1093–1100.
7. Rouzina, I.; Bloomfield, V.A., Heat Capacity Effects on the Melting of DNA. 1. General Aspects, *Biophysics* J., **1999**, 77, 3242–3251.
8. Topala, T.; Bodoki, A.; Oprean, L.; Oprean, R., Experimental Techniques Employed in the Study of Metal Complexes-DNA–Interactions, *Farmacia*, **2014**, 62, 1049–1061.
9. Tataurov, Andrey V., Yong You, and Richard Owczarzy. Predicting ultraviolet spectrum of single stranded and double stranded deoxyribonucleic acids, *Biophys. Chem.*, **2008**, 133, 1-3, 66–70.
10. Lando, D.Y.; Fridman, A.S.; Chang, C-.L.; Grigoryan, I.E.; Galyuk, E.N.; Murashko, O.N.; Chen, C-.C.; Hu, C-.K., *Anal. Biochem.*, **2015**, 479
11. Rouzina, I.; Bloomfield, V.A., Heat Capacity Effects on the Melting of DNA. 2. Analysis of Nearest-Neighbor Base-Pair Effects, *Biophysics J.*, **1999**, 77, 3242–3251.
12. Assi, H.A.; Garavis, M.; Gonzalex, C.; Damha, M.J., i-Motif DNA: Structureal Features and Significance to Cell Biology, *Nucleic Acids Res.*, **2018**, 16, 8038–8056.
13. Tibanyenda, N.; De Bruin, S.H.; Haasnoot, C.A.; Van der Marel, G.A.; Van Boom, J.H., Hilber, C.W., The EFFECT OF Single Base-Pair Mismatches on the Diplex Stability of d(T-A-T-T-A-A-T-A-T-C-A-A-G-T-T-G) d(C-A-A-C-TT-G-A-T-A-T-T-A-A-T-A). *Eur. J. Biochem.*, **1984**, 139, 12–27.
14. Singh, A.; Singh, N., Effect of Salt Concentration on the Stability of Heterogeneous DNA, Physica A, **2015**, 319, 328–334.
15. Schildkraut, C.; Lifson, S., Dependence of the Melting Temperature of DNA on Salt Concentration, *Biopolymers*, **1965**, 3, 195–208.
16. Bjorndal, M.T.; Fygenson, K., DNA Melting in the Presence of Fluorescent Intercalating Oxazole Yellow Dyes Measured with a Gel-Based Assay, Biopolymers: Original Research on Biomolecules, **2002**, 65, 40–44.
17. Dragan, A.I.; Pavlovis, R.; McGivney, J.B.; Casas-Finet, J.R.; Bishop, E.S.; Strouse, R.J.; Schenerman, M.A.; Geddes, C.D., SYBR GreenI: Fluorescence Properties and Interaction with DNA, J. *Fluoresc.*, **2012**, 22, 1189 – 1199.

Learn more at **thermofisher.com/evolution**